

SUPPLEMENTARY INFORMATION

Direct observation of dislocation motion in the complex alloy T-Al-Mn-Fe using in-situ transmission electron microscopy

Marc Heggen, Michael Feuerbacher, Rafal E. Dunin-Borkowski

Ernst Ruska-Centre for Microscopy and Spectroscopy with Electrons,

Forschungszentrum Jülich GmbH,

D-52425 Jülich, Germany

The T-Phase and the structure of MD defects: T-Al₃Mn and its isostructural ternary extensions T-Al-Mn-Fe and T-Al-Mn-Pd are CMAs with 156 atoms per unit cell, an orthorhombic structure (space group Pnma), and with lattice parameters $a = 1.48$ nm, $b = 1.24$ nm and $c = 1.25$ nm [1–5]. Figure 1 a shows a representation of the T-Al-Mn-Pd unit cell (blue rectangle) projected along $[0\ 1\ 0]$ [6,7]. The T-phase is often represented by structural subunits in the form of area-filling, elongated hexagon tiles (white and yellow polygons in Figure 1 a), arranged in rows of alternating orientation. This tiling representation is superimposed to a high-resolution high-angle annular dark field (HAADF)-STEM image of the T-Al-Mn-Pd phase at the right-hand side of Figure 1a. Figure 1 b shows a HAADF-STEM image of a MD in T-Al-Mn-Pd[6], the core of which is represented by a green polygon. Motion of the MD – in this example from right to left – is escorted by bow-tie shaped tiles (red), which change the stacking sequence of the hexagons in front of the core. The bow-tie shaped tiles represent defects characteristic for CMAs and quasicrystals, referred to as phason defects or phasons. Phasons are linear defects that do not involve a strain field but refer to local deviations from the ideal structure that can be represented by a rearrangement of tiles.

In its wake the MD trails a (1 0 0) planar defect, which can be described as a slab of R-phase, and is represented by a parallel arrangement of hexagonal tiles. It is a characteristic feature of MDs that in a given structure they exist in variants with different Burgers vector length. The Burgers vector lengths of the variants are scaled by powers of τ , the number of the golden mean, i.e. they represent hierarchies of irrational partial dislocations in the structure. The MD shown in Fig. 1b has a $-\tau^{-4}c[0 \ 0 \ 1]$ Burgers vector (red arrow in Figure 1b), where τ is the number of the golden mean. This Burgers vector lies in the plane of motion, i.e. the MD moves by pure glide and creates a (0 0 1) stacking fault in its wake. MDs moving by other types of motion, i.e. by pure climb or mixed glide/climb were observed in T-Al-Pd-Mn and other CMA structures[7,8].

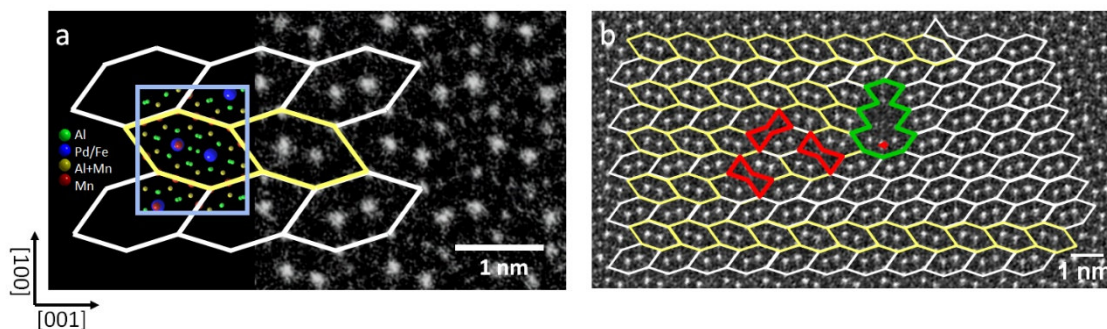


Figure S1 a) Structure model and high-resolution HAADF-STEM micrograph of T-Al-Mn-Pd/Fe along the [0 1 0] direction. Atom positions are represented by blue (Pd or Fe), red (Mn), green (Al), and olive spheres (mixed Al and Mn occupation). The unit cell is outlined by a blue rectangle. White and yellow hexagons are used as a tiling representation. b) HAADF-STEM micrograph of a MD (green polygon) with a (1 0 0) planar defect represented by a parallel arrangement of hexagons (white hexagons at the right). The MD core is escorted by phason defects (red bow-tie shaped tiles).

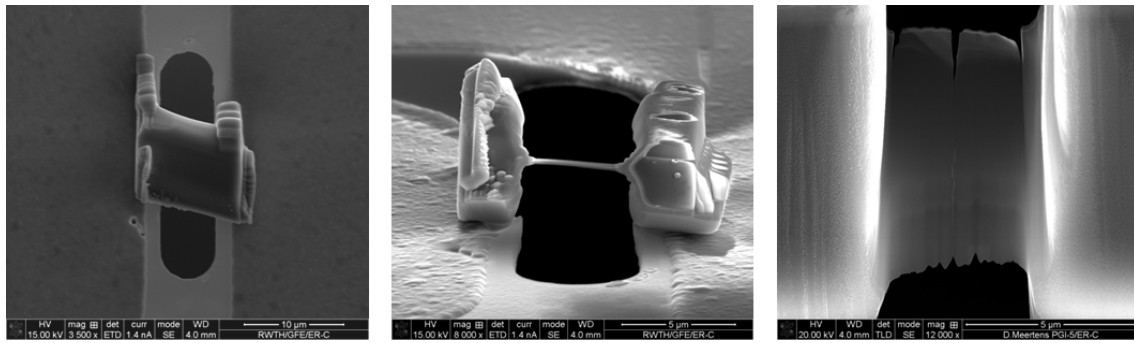


Figure S2: Scanning electron micrographs of the T-Al-Pd-Fe deformation sample during different stages of the FIB preparation process.

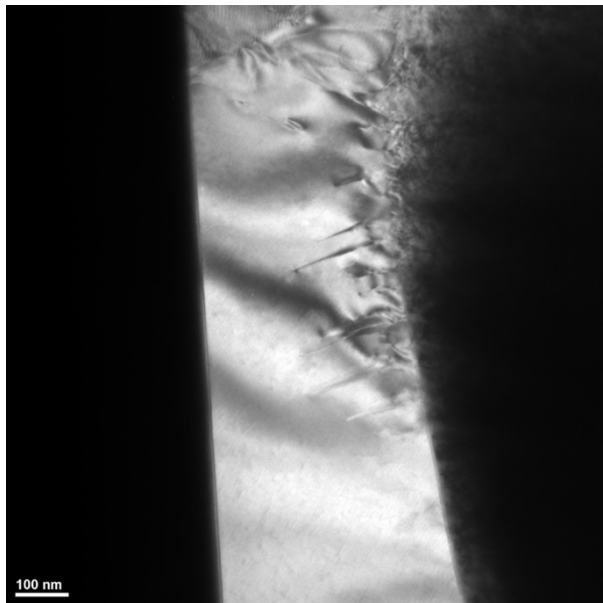


Figure S3: Dark-field TEM image of dislocations and stacking faults, created at the edge of the FIB lamella.

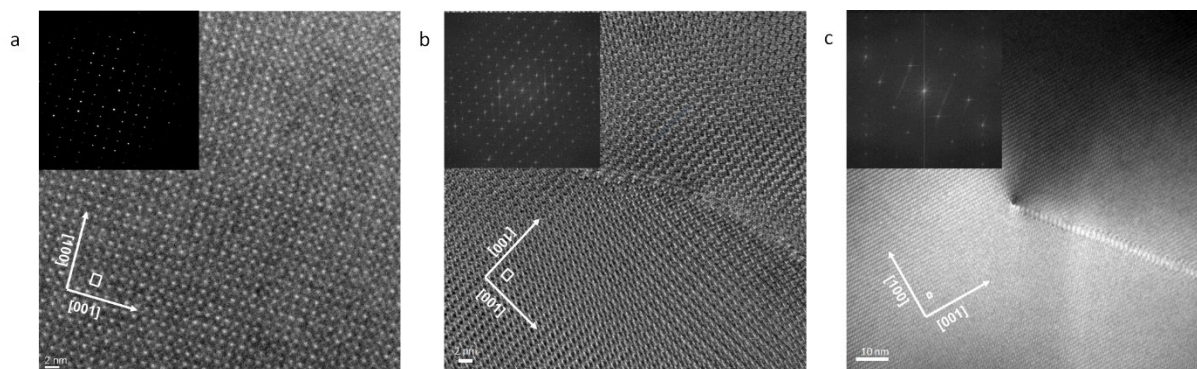


Figure S4: a) High-resolution TEM image of the T-Al-Pd-Fe structure and corresponding electron-diffraction image of the sample area. b) High-resolution TEM image of a defect in T-Al-Pd-Fe taken from the image series in Figure 2 and movie 2 and corresponding fast-Fourier-transform image obtained on an FEI TITAN microscope. b) High-resolution TEM image of a defect in T-Al-Pd-Fe taken from movie 4 and corresponding fast-Fourier-transform image obtained. White rectangles indicate the unit cell.

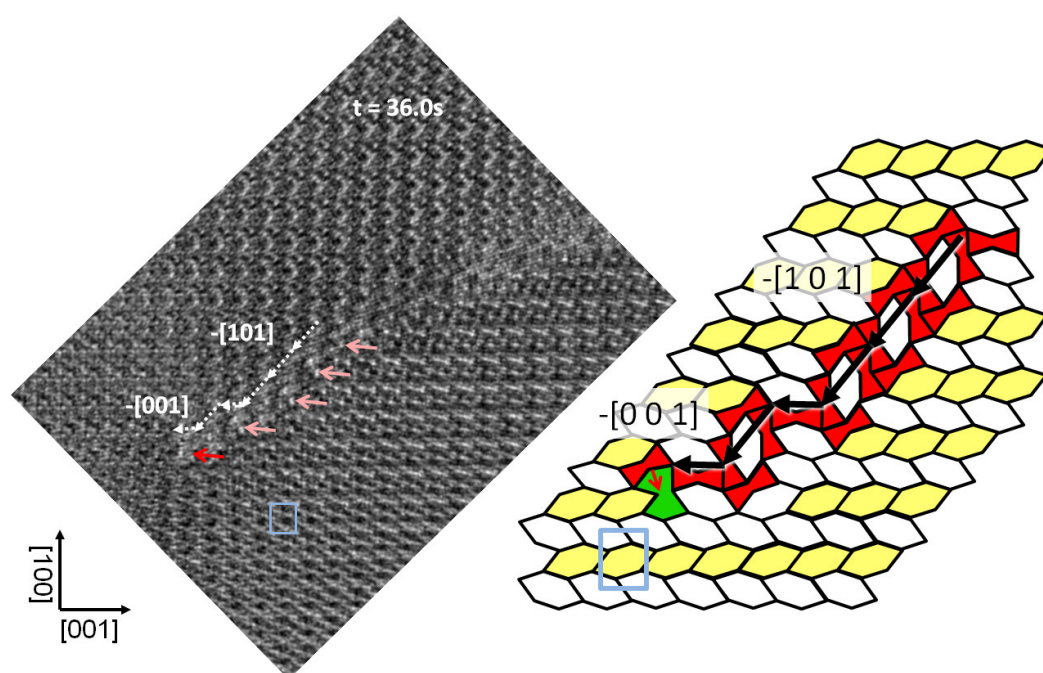


Figure S5: a) High-resolution TEM image of the in-situ heating experiment (Figure 2 a) in comparison with tiling model of the alternating motion along $-[1\ 0\ 1]$ and $-[0\ 0\ 1]$ direction. The unit cell is indicated by a blue rectangle.

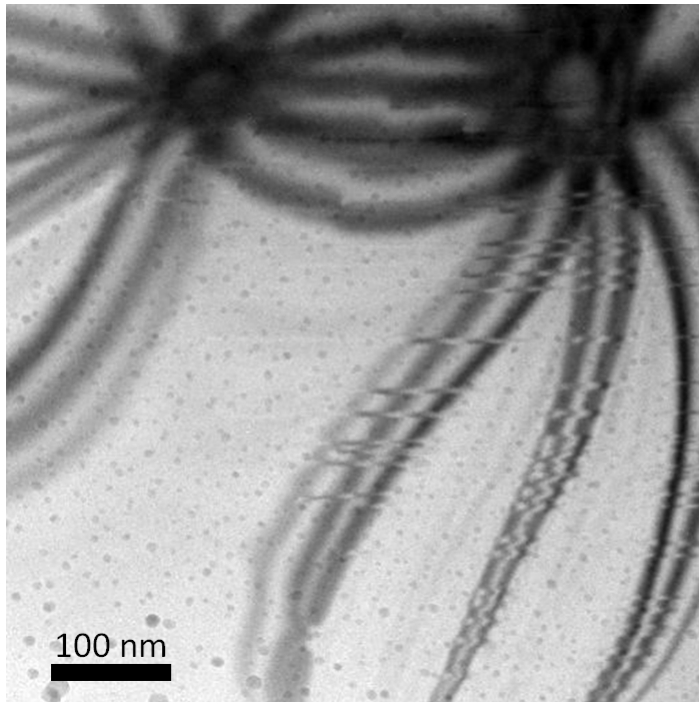


Figure S6: a) Bright-field TEM image showing stacking faults and demonstrating the typical strong bending of the FIB lamella sample during in-situ heating.

Movie 1 was taken at 645°C under Bragg-contrast conditions on a FEI Tecnai F20. The edge length of the image frame is 500nm. The image frequency is 0.67 frames/s.

Movie 2 & 3 were taken at 565°C on a image-corrected FEI TITAN. The image frequency is 0.31 frames/s

Movie 4 was taken at 640°C on a FEI Tecnai F20. The edge length of the image frame is 145nm. The image frequency is 1.1 frames/s.

Movie 5a & 5b illustrate a single step of motion of the MD shown in Figure 4a. The animation uses two superimposed HAADF-STEM images shifted by one lattice constant.

References

- [1] Taylor MA. The space group of $MnAl_3$. *Acta Cryst.* 1961;14:84–84.
- [2] Hiraga K, Kaneko M, Matsuo Y, et al. The structure of Al_3Mn : Close relationship to decagonal quasicrystals. *Philosophical Magazine B.* 1993;67:193–205.
- [3] Klein H, Boudard M, Audier M, et al. The T- Al_3 (Mn, Pd) quasicrystalline approximant: Chemical order and phason defects. *Philosophical Magazine Letters.* 1997;75:197–208.
- [4] Balanetskyy S, Meisterer G, Heggen M, et al. Reinvestigation of the Al–Mn–Pd alloy system in the vicinity of the T- and R-phases. *Intermetallics.* 2008;16:71–87.

- [5] Pavlyuchkov D, Balanetsky S, Kowalski W, et al. Stable decagonal quasicrystals in the Al-Fe-Cr and Al-Fe-Mn alloy systems. *Journal of Alloys and Compounds*. 2009;477:L41–L44.
- [6] Heggen M, Houben L, Feuerbacher M. Plastic-deformation mechanism in complex solids. *Nature Mater*. 2010;9:332–336.
- [7] Heggen M, Houben L, Feuerbacher M. Metadislocations in the complex metallic alloys T–Al–Mn– (Pd, Fe). *Acta Materialia*. 2011;59:4458–4466.
- [8] Feuerbacher M, Heggen M. Chapter 94 Metadislocations. In: Hirth JP, Kubin L, editors. *Dislocations in Solids* [Internet]. Elsevier; 2010 [cited 2022 Aug 18]. p. 109–170. Available from: <https://www.sciencedirect.com/science/article/pii/S1572485909016039>.